

# Surface ozone concentrations in Agra: links with the prevailing meteorological parameters

Vyoma Singla · Tripti Pachauri · Aparna Satsangi ·  
K. Maharaj Kumari · Anita Lakhani

Received: 26 April 2011 / Accepted: 8 March 2012 / Published online: 30 March 2012  
© Springer-Verlag 2012

**Abstract** Measurements of surface ozone ( $O_3$ ), nitric oxide (NO), nitrogen dioxide ( $NO_2$ ), oxides of nitrogen ( $NO_x=NO+NO_2$ ) and meteorological parameters have been made at Agra (North Central India,  $27^{\circ}10'N$ ,  $78^{\circ}05'E$ ) in post monsoon and winter season. The diurnal variation in  $O_3$  concentration shows daytime in situ photochemical production with diurnal maximum in noon hours ranging from 51 to 54 ppb in post monsoon and from 76 to 82 ppb in winter, while minimum (16–24 ppb) during nighttime and early morning hours. Average 8-h  $O_3$  concentration varied from 12.4 to 83.9 ppb. The relationship between meteorological parameters (solar radiation intensity, temperature, relative humidity, wind speed and wind direction) and surface  $O_3$  variability was studied using principal component analysis (PCA), multiple linear regression (MLR) and correlation analysis (CA). PCA and MLR of daily mean  $O_3$  concentrations on meteorological parameters explain up to 80 % of day to day ozone variability. Correlation with meteorology is strongly emphasized on days having strong solar radiation intensity and longer sunshine time.

## 1 Introduction

Ozone is one of the important trace gases in the troposphere. Tropospheric ozone is a secondary pollutant formed by a series of photochemical reactions from  $NO_x$  (oxides of nitrogen) and volatile organic compounds (VOCs) in the presence of solar radiation. It constitutes only 10 % of the total ozone in the atmosphere but is the main photochemical precursor of the hydroxyl radical (OH) which is the most active daytime oxidant in the troposphere (Bai 2010). Hence, absorption of light in the near-ultraviolet (UV) region (i.e.,  $\lambda=290\text{--}310$  nm) by ozone molecules initiates free radical chain reactions which oxidize many trace gases such as CO,  $CH_4$ , VOCs, which otherwise would act as efficient greenhouse gases. Moreover,  $O_3$  is a greenhouse gas by absorbing infrared, thus contributing to climate change (Wilson et al. 2007; Judith et al. 2008; Son et al. 2008). Surface ozone levels and its changes are of great interest since harmful effects of  $O_3$  and positive trends of its concentration were established at a number of northern hemispheric locations (Scheel et al. 1997; Roemer and Tarasova 2002). The relation between reactants and products can be analyzed by systematically monitoring  $O_3$  and  $NO_x$ .

The changes in local meteorological conditions, such as wind direction, wind speed, relative humidity, and temperature, can greatly affect chemical ozone generation, dispersion and deposition on the surface causing variations in ozone concentrations (Duenas et al. 2002; Elminir 2005; Khiem et al. 2010). Therefore, analysis of the influences of the changes in meteorological conditions on variations in ozone is very helpful for better understanding variations in ozone concentrations. In recent years, meteorological effects on variations in surface ozone concentrations have been extensively studied (Tarasova and Karpetchko 2003; Tu et al. 2007; Cheng et al. 2007). These studies have shown that meteorological conditions can have significant impacts upon

V. Singla · T. Pachauri · A. Satsangi · K. M. Kumari ·  
A. Lakhani (✉)  
Department of Chemistry, Faculty of Science,  
Dayalbagh Educational Institute,  
Dayalbagh, Agra 282110, India  
e-mail: anita.lakhani01@gmail.com

V. Singla  
e-mail: s.vyoma@gmail.com

T. Pachauri  
e-mail: triptipachauri09@gmail.com

A. Satsangi  
e-mail: srivastava\_aparna@yahoo.com

K. M. Kumari  
e-mail: maharajkumari.k@rediffmail.com

surface ozone concentrations. For instance, ozone levels tend to be higher under hot, sunny conditions favourable for photochemical ozone production in the presence of precursors. At the same time, higher temperatures cause convection to develop, which in turn can enhance vertical ozone transport. Conversely, wet, rainy weather with high relative humidity is typically associated with the low ozone levels provided by less intensive photochemical production and, possibly, by ozone deposition on water droplets (Lelieveld and Crutzen 1990). Windy weather can influence ozone concentration near the surface in a different way. Tarasova and Karpetchko (2003) investigated the relationship between local meteorological conditions and the availability in surface ozone at Lovozero (Kola Peninsula) for the period of 1999–2000 and found that 70 % of the day-to-day ozone variability could be explained by changes in temperature, relative humidity, and wind speed.

The results of investigation in Western Europe showed that the parameters of major importance for the occurrence of photochemical ozone are meteorological parameters (Andric et al. 2009). The studies conducted in Germany indicate that meteorological conditions have a decisive impact on surface ozone concentrations (Spichtinger et al. 1996; Andric et al. 2009). Broniman and Neu (1997) found that at favourable meteorology (high solar radiation, high temperatures, low wind speeds) ozone production dominates at both, urban and rural sites in Switzerland, and additionally, weekly cycles of ozone peaks change with meteorology. Khiem et al. (2010) and Andric et al. (2009) discussed the relationship between changes in meteorological conditions and variation in ozone levels by time series analysis and multivariate statistical methods. Similarly, the effect of meteorological parameters on ozone production at this site was studied using multiple linear regression (MLR) and principal component analysis (PCA). PCA is used as an exploratory tool to discern the variables contributing to the concentration of any chemical specie at a particular site. It is a method used to project the variations in a multivariate data matrix  $\mathbf{X}$  with  $n$  rows (objects) and  $k$  columns (variables) into a few uncorrelated or orthogonal principal components (PCs) (Jackson 1991). Basically, the systematic variation of the  $\mathbf{X}$  matrix is extracted into the smaller matrices, the score  $\mathbf{T}$  and the loading  $\mathbf{P}$  matrices. Thus, the principle of PCA is to transform the original set of variables into a smaller set of linear combinations that account for most of the variance of the original data set. The primary function of this analysis is the reduction of the number of variables while retaining the original information as much as possible, and thus variables with similar characteristics can be grouped into factors (Ho et al. 2002). The first PC is oriented to explain as much variation in the data as possible and presents the best linear summary of  $\mathbf{X}$ . The second PC is orthogonal to the first, and explains the next largest variation in the data, and so forth. The PCs of the  $\mathbf{T}$  matrix can be plotted in two-dimensional space to produce score plots. In a score plot, the relationship between objects is visualized, hence two

objects close to each other in the score plot are similar and vice versa. The loading plots of the  $\mathbf{P}$  matrix are produced in the same way and visualize how the variables are related to each other. Comparison of score and loading plots reveals the relationship between the objects and the variables, e.g., which species is present in high or low concentrations at the sampling site as positioned in different parts of the score plot.

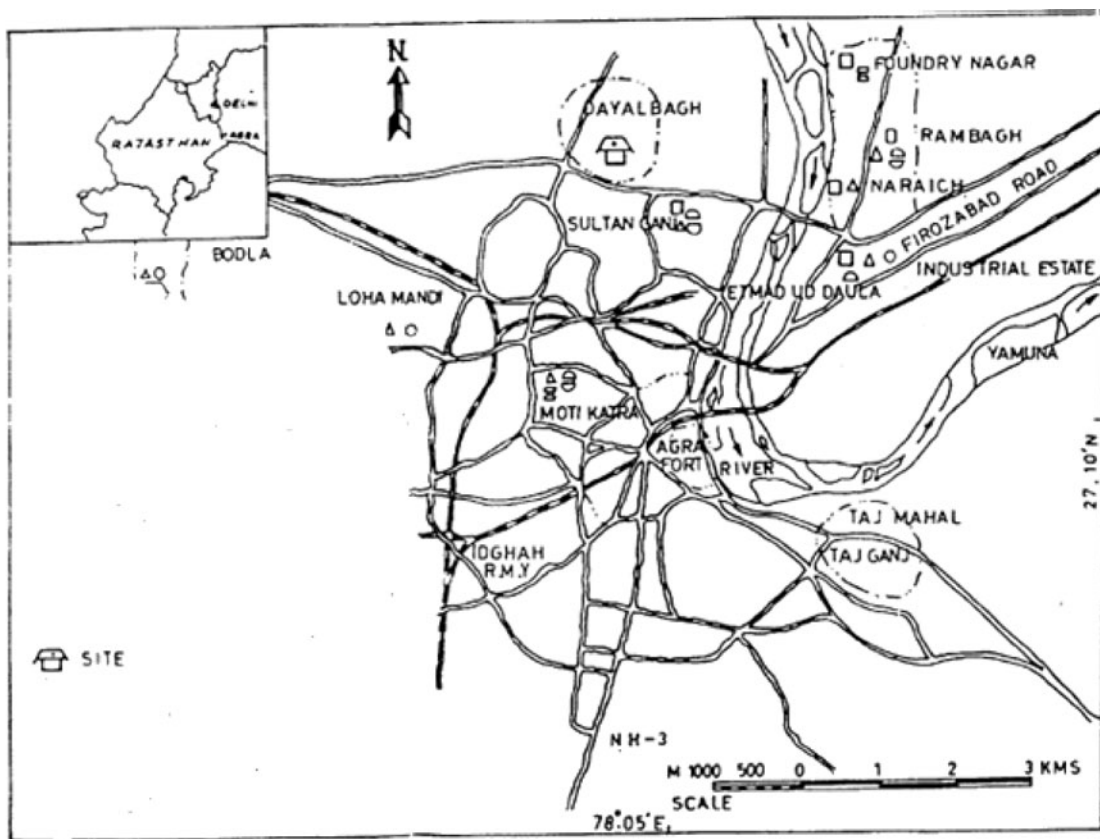
These techniques are known to be powerful tools used in analysing environmental data and to reveal the similarities among variables and cases (Statheropoulos et al. 1998; Lengyel et al. 2004; Felipe-Sotelo et al. 2006; Karatzas and Kaltsatos 2007). In this study, measurements of surface  $\text{O}_3$  and  $\text{NO}_x$  were done in the months of September 2010 to January 2011. The period covering September 2010 to October 2010 is taken as representative months for post monsoon while November 2010 to January 2011 represents winter season. In view of the fact that monsoon offsets in August and an unexpected rain event was observed in September 2010, September and October 2010 represents post monsoon season. Hence, this study was planned to assess the photochemical production of ozone and monitor different meteorological parameters like temperature, solar radiation, wind speed, wind direction and relative humidity contributing important role in its formation.

## 2 Materials and methods

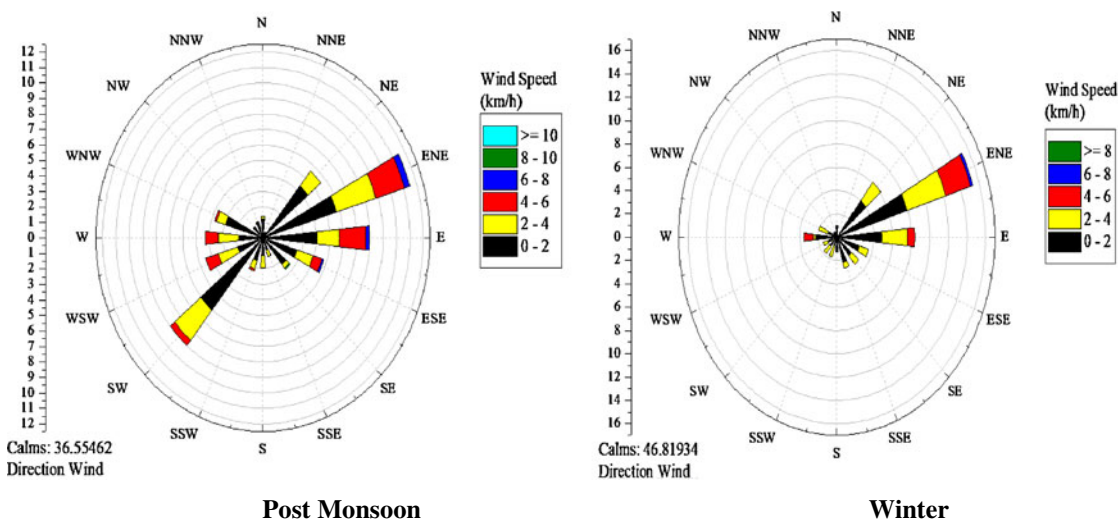
### 2.1 Site description

The sampling site is located in Agra (North Central India, 27 °10'N, 78 °05'E). It lies in a the semi-arid zone, adjacent to the Thar Desert of Rajasthan. Industrial activities of Agra include rubber processing, lime processing, engineering and a few ferrous casting industries based on natural gas. Apart from the local sources, Mathura refinery and Firozabad glass industries are both situated at a distance of 40 km from Agra. Agra has continental type of climate. The city observes dry climate during summer and winter. Annual rainfall is about 650 mm with 90 % being received during the monsoon season (July–August). Winter is associated with calm periods of about 48 %.

The study was carried out at Dayalbagh Educational Institute Campus in Dayalbagh, which lies towards north of Agra city. It is a small suburban site with no industrial activity around. Dayalbagh is a small residential community lying immediately outside the city where agricultural activities predominate. The meteorology of Agra is such that prevailing winds are mostly from the northwest so that Mathura lies upwind while Firozabad downwind. Population around the sampling site is about 25,000. The sampling site lies by the side of a road that carries mixed vehicular traffic, moderate (of the order of 1,000 vehicles) during the day and minimal (of the order of 100 vehicles) at night. The campus lies about 2 km north of the National Highway-2 (NH-2) which has dense vehicular traffic



(a) Geographical Map of Agra



(b) Prevailing wind pattern at Agra

Fig. 1 a Geographical map of Agra. b Prevailing wind pattern at Agra

( $10^6$  vehicles) throughout the day and night. Figure 1a and b shows the geographical map and the prevailing wind pattern at sampling site, respectively. The temperature profile during post

monsoon varied from 22 to 30 °C, while in winter it varied from 1 to 15 °C. The rainfall observed during post monsoon was 166 mm with the maximum relative humidity reaching up to 94 %.

## 2.2 Instrumentation and methodology

Surface O<sub>3</sub> and NO<sub>x</sub> concentrations were recorded using continuously operating O<sub>3</sub> analyzer (Thermo Fischer Model 49i) and NO<sub>x</sub> analyzer (Thermo Fischer Model 42i) in post monsoon and winter season. The air samples were drawn at the height of 15 m above the ground level through sampling hood. The ozone concentration measurement is based on UV absorption photometry, resting upon absorption of radiation of wavelength 254 nm by ozone in the analyzed sample. The radiation source is a UV lamp and clean air (zero) and the sample itself are alternately measured in cells. The analyzer incorporates corrections due to changes in temperature, pressure in the absorption cell and drift in the intensity of the UV lamp. This method with automatic pressure and temperature compensation meets the challenging requirements for O<sub>3</sub> measurements. Calibration of the system was done regularly with the help of a built-in ozone generator. Zero setting of the analyzer was also performed regularly by admitting zero air (free of ozone) into the analyzer. The O<sub>3</sub> analyzer is designed such that the wavelength at which light is emitted by UV mercury lamp is equivalent to the wavelength at which it absorbs ozone, i.e., 253.7 nm. The calibration is carried out by matching the preset values in the analyzer with the current applied to the UV lamp. The detector is employed before and after the absorption takes place in the fixed length flow path, so the variations in the intensity of the light are balanced. The minimum detection limit and precision of the analyzer is 0.5 and 1 ppb, respectively.

The NO<sub>x</sub> analyzer is based on the chemiluminescence effect of NO<sub>2</sub> produced by the oxidation of NO by O<sub>3</sub> molecules, which peaks at 630 nm radiation. In this analyzer, NO<sub>2</sub> is measured by converting it into NO using the thermal conversion (heated molybdenum) method. The molybdenum converter is found to have higher sensitivity and ~100 % conversion efficiency (Finlayson-Pitts and Pitts 1986). But it has been realized that molybdenum converter also converts other species such as PAN, HNO<sub>3</sub>, other organic nitrates and nitrites into NO (Winer et al. 1974). However, these concentrations may be very small at the surface levels. Thus, the actual concentrations of NO<sub>2</sub> and therefore NO<sub>x</sub> might be lower. The minimum detection limit and precision of NO<sub>x</sub> analyzer is 0.4 and 1 ppb, respectively. Calibration for NO<sub>2</sub> was done by using permeation tube (KINTEK, Texas).

The online O<sub>3</sub> and NO<sub>x</sub> analyzers records concentration on an averaging time of every 5 min. The 5-min average concentrations were further averaged to get 1-h average O<sub>3</sub> and NO<sub>x</sub> concentration. Different meteorological parameters like temperature, relative humidity, wind speed and wind direction were recorded using Wind Monitor WM271 Data Logger. The data logger gives reading at every second which was further averaged to get 1-h average value.

## 3 Results and discussion

The concentration of O<sub>3</sub> at any site depends on the photochemical production of O<sub>3</sub> related mainly to NO<sub>x</sub> concentration, local meteorological conditions and long range transport. These effects can be visualized by studying the diurnal and seasonal variations.

### 3.1 Day-to-day variation

Figure 2 shows the average O<sub>3</sub> and NO<sub>x</sub> concentration in post monsoon and winter season on a day-to-day basis at this site. As expected, the variation in O<sub>3</sub> shows a direct and potential link with NO<sub>x</sub>. The variation in O<sub>3</sub> concentration was observed to vary proportionally with the sunshine hours and temperature variability while NO<sub>x</sub> concentration peaks during early morning and late evening hours and hence shows direct link with traffic rush hours throughout the study period. In post monsoon, O<sub>3</sub> concentration varied from 62 to 70 ppb and 2 to 10 ppb for NO<sub>x</sub> in the daytime while in the nighttime, the concentration was observed to vary from 4 to 12 ppb (O<sub>3</sub>) and from 18 to 20 ppb (NO<sub>x</sub>), respectively. In winter season, the daytime concentration was observed to vary from 45 to 53 ppb (O<sub>3</sub>) and from 4 to 14 ppb (NO<sub>x</sub>) and nighttime and early morning concentration varied from 15 to 21 ppb (O<sub>3</sub>) and 20 to 24 ppb (NO<sub>x</sub>).

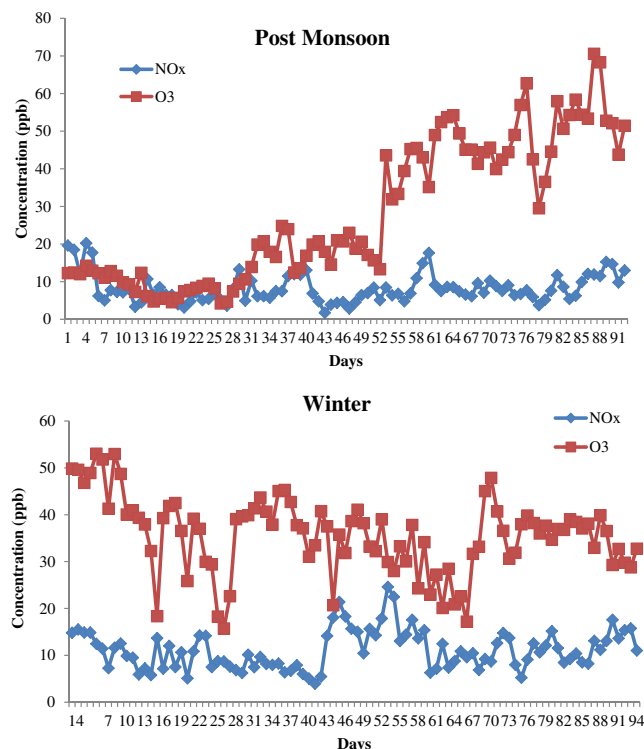


**Fig. 2** Day-to-day variation of O<sub>3</sub> and NO<sub>x</sub> concentration in post monsoon and winter

The higher concentrations of O<sub>3</sub> during daytime correspond to photochemical production and higher concentration of NO<sub>x</sub> in the morning and evening hours corresponds to traffic rush hours. With the offset of monsoon, in post monsoon season as intensity of solar radiation start increasing, O<sub>3</sub> concentration increases gradually from 20 to 49 ppb in September and from 45 to 70 ppb in October. In post monsoon, a sudden marked decrease in O<sub>3</sub> and NO<sub>x</sub> concentration was observed on September 19, 20, and 21, 2010. These days were observed to experience heavy rain (45.5 mm on September 19, 29.5 mm on September 20 and 37.5 mm on September 21), which lowered the O<sub>3</sub> concentration to as low as from 13 to 17 ppb and NO<sub>x</sub> concentration ranges from 6 to 11 ppb. High precipitation and wash-out effects with no sunshine leads to lowering of O<sub>3</sub> and NO<sub>x</sub> concentration. Again, with the onset of solar radiation, O<sub>3</sub> concentration started increasing gradually and reached maximum up to 48.9 ppb. On the other hand, in winter season O<sub>3</sub> concentration showed linear relationship with solar radiation intensity and sunshine. The average daytime concentration varied from 45 to 70 ppb.

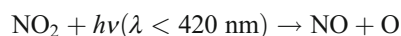
The Environmental Protection Agency (EPA) has set the critical 8-h O<sub>3</sub> standard as 75 ppb which states that any 8-h average O<sub>3</sub> concentration should not exceed 75 ppb. The 8-h average O<sub>3</sub> concentration was calculated during the study period from 09:00 to 17:00 hours considering that maximum formation of O<sub>3</sub> takes place during daytime. The 8-h average O<sub>3</sub> concentration varied from as low as 12.4 ppb to as high as 75.6 ppb in post monsoon and 15.7 ppb to 83.9 ppb in winter. It is expected that variation in meteorological conditions during the study period results in variation of 8-h average O<sub>3</sub> concentration on each day. The 8-h average O<sub>3</sub> concentration at this site lies below the critical level as set by EPA on maximum number of days although few days were observed to experience high levels, lying very close to the critical standard. A similar result has also been reported by Pudasainee et al. (2006) in Kathmandu valley, Nepal, from November 2003 to October 2004.

### 3.2 Diurnal and seasonal variations

The variation of surface O<sub>3</sub> within a day may be helpful in delineating the processes responsible for O<sub>3</sub> formation at a particular site. The hourly average diurnal variation of O<sub>3</sub> in post monsoon and winter season is represented in Fig. 3. As expected, the time concentration profiles of O<sub>3</sub> follow the close relationship with the diurnal cycle of solar radiation time. The diurnal variation in O<sub>3</sub> shows the daytime in situ photochemical production with diurnal maximum in noon hours (13:00–15:00 hours in post monsoon and 14:00–16:00 hours in winter) and minimum during nighttime and early morning hours. However, the NO<sub>x</sub> concentration

shows a sharp increase and reaches maximum (20–24 ppb) at a time that coincides with the maximum automobile traffic in the morning and evening and thus follows an inverse relationship with O<sub>3</sub>.

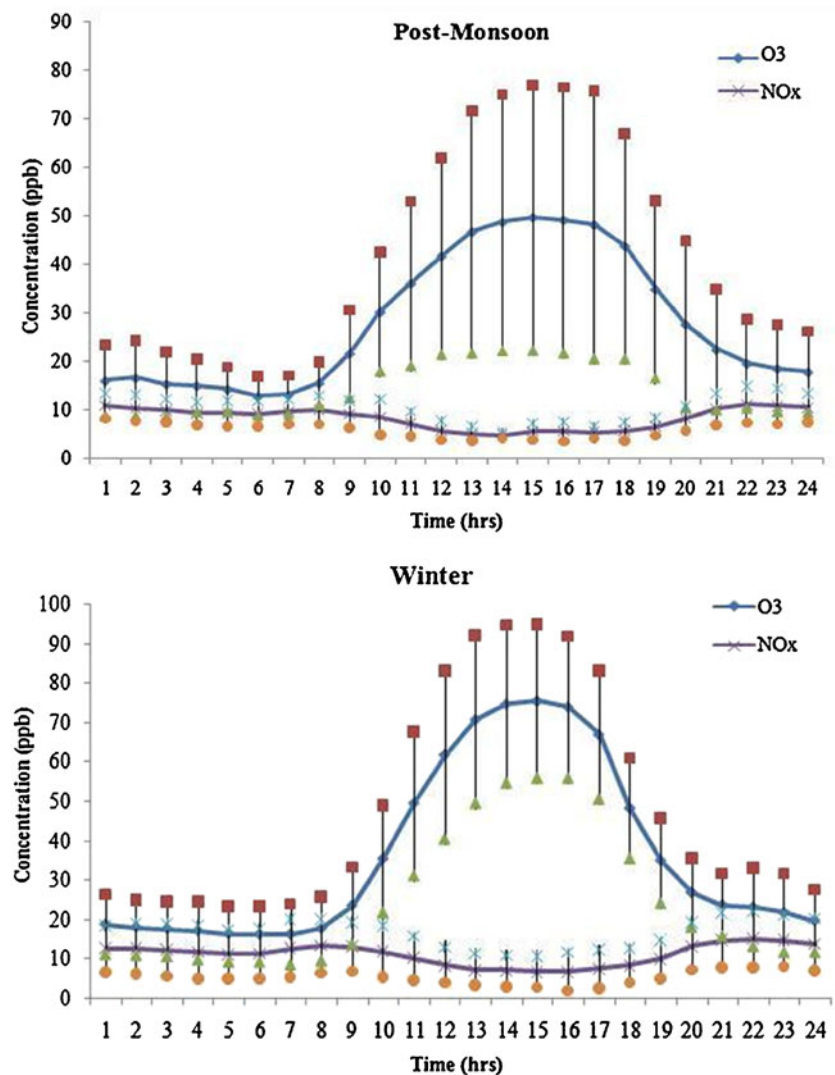
The average O<sub>3</sub> concentration in the early morning hours (01:00–09:00 hours) was almost similar in post monsoon and winter season ranging from 13 to 21 ppb. With the onset of solar radiation, the concentration started increasing gradually as a result of photochemical build-up of O<sub>3</sub> probably due to its formation through photolysis of NO<sub>2</sub> via following set of reactions:



The maximum O<sub>3</sub> concentration was observed during noon hours ranging from 51 to 54 ppb (13:00–15:00 hours) in post monsoon and from 76 to 82 ppb (14:00–16:00 hours) in winter. The maximum concentration during noon hours might be due to the additional production of O<sub>3</sub> by photo-oxidation of precursor gases, like CO, CH<sub>4</sub>, and other hydrocarbons in the presence of sufficient amount of NO/NO<sub>x</sub>. The concentration of O<sub>3</sub> was observed to be comparatively higher in winter than during post monsoon. Intensity of solar radiation and sunshine hours are the principal factors governing the formation of O<sub>3</sub>. The intensity of solar radiation (37–53 W m<sup>-2</sup> in winter and 30–51 W m<sup>-2</sup> in post monsoon) and sunshine time (10:00–18:00 hours in post monsoon and 10:00–17:00 hours in winter) were more or less similar during the two seasons and hence does not account for higher concentration of O<sub>3</sub> in winter. Thus, the only plausible reason responsible for higher concentration in winter might be the temperature inversion effect in atmospheric boundary layer resulting in trapping of O<sub>3</sub> near the Earth's surface (Lal et al. 2000). In post monsoon, blowing winds might also result in dispersion of O<sub>3</sub>.

The NO<sub>x</sub> maximum was observed in the late evening hours when O<sub>3</sub> concentration gradually falls with the diminishing of solar radiation and its depletion via: O<sub>3</sub> + NO → NO<sub>2</sub> + O<sub>2</sub>. This reaction of NO with O<sub>3</sub> with a reaction rate of 10<sup>8</sup> s<sup>-1</sup> is about 2 orders faster than any other chemical loss reactions. The nighttime O<sub>3</sub> concentrations are observed to be almost similar in post monsoon and winter season and vary from 16 to 24 ppb. In the evening, a secondary NO<sub>x</sub> maximum (24.5 ppb) was observed corresponding to traffic rush hours during which time O<sub>3</sub> exhibits a secondary minimum (11.3 ppb). The concentration of NO<sub>x</sub> was observed to be little bit lower in post monsoon (12.2 ppb) as compared to winter (23.4 ppb). The lower concentrations could be due to draining out of pollutants with rain. Comparatively higher concentrations in winter might be attributed to the stable weather conditions

**Fig. 3** Diurnal variation of O<sub>3</sub> and NO<sub>x</sub> concentration in post monsoon and winter



which cause the pollution to rise. A diurnal pattern with maximum ozone concentration during daytime and minimum during nighttime is also observed at Pune, Mahabaleshwar, Joharapur, Mulanagar and Bhenda by Debaje and Kakade (2009), Ahmedabad by Lal et al. (2000) and Gadanki by Naja and Lal (2002). The variation of O<sub>3</sub> and NO<sub>x</sub> throughout the study period is also represented as a contour plot in Fig. 4.

To evaluate surface ozone variations related to the variability of local meteorological parameters, multivariate statistical methods like PCA, MLR and correlation analysis (CA) were carried out. In situ photochemical production, deposition and long range transport of O<sub>3</sub> are all driven by local meteorology. Hence, temperature, solar radiation, wind speed and wind direction were chosen as variables for this analysis. These variables were considered to be complementary as they influence ozone formation through different processes.

### 3.3 Principal component analysis

The technique, PCA was applied to the identify groups of correlated variables, like meteorological parameters and precursors, contributing to the concentration of O<sub>3</sub>. Interpretation of the results of PCA is carried out by visualization of the component scores and loadings. Before subjecting the data to PCA, a pretreatment involving an autoscaling of the data was performed. In this autoscaling procedure all variables were mean centered and scaled to unit variance, by subtracting the mean  $\bar{x}_j$  of each variable  $j$  from the result  $x_{ij}$  of each sample  $i$  for that variable and dividing the result by the standard deviation  $s_j$  of that variable. The resulting autoscaled  $z_{ij}$  were used instead of the original  $x_{ij}$ .

$$z_{ij} = (x_{ij} - \bar{x}_j) / s_j$$

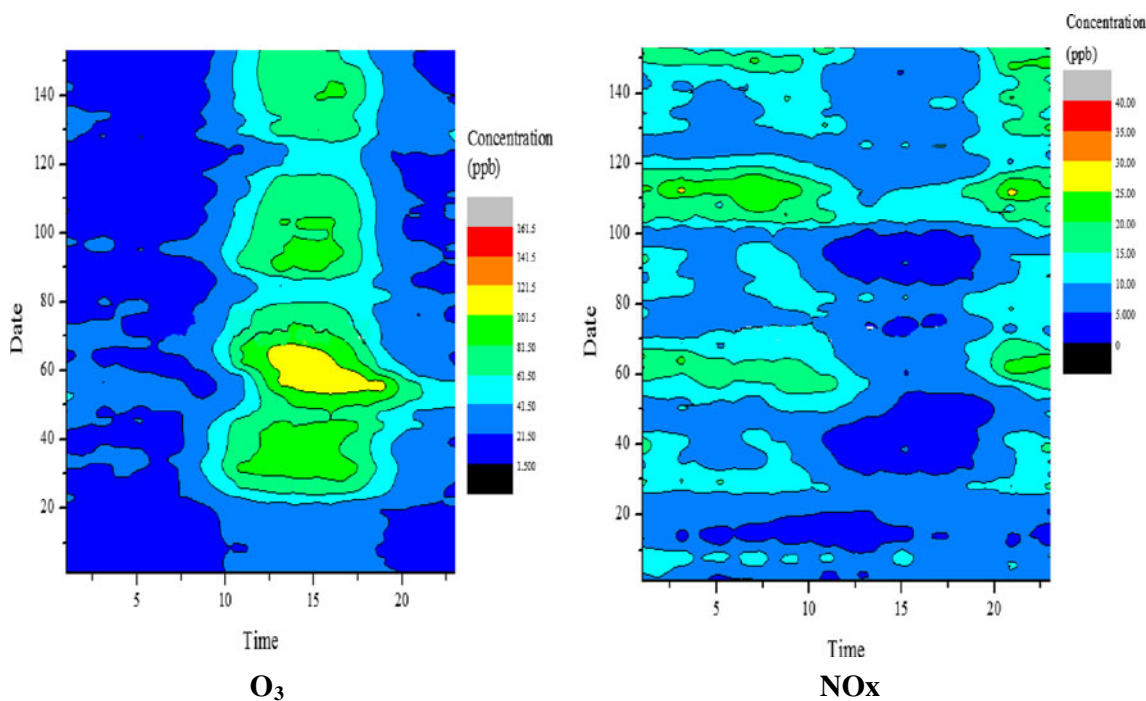


Fig. 4 Contour plots of O<sub>3</sub> and NO<sub>x</sub>

As a result of this autoscaling, each variable has about the same range and it is avoided that some variables would be more important than others because of scale effects.

In this study, PCA was done using Statistical Package for Social Science (SPSS, version 16.0) by adopting varimax procedure for rotation of factor matrix into one that was easier to interpret. The number of factors to be retained was decided on the basis of the breaks in the slopes of scree plots that are plots between eigenvalues and PCs. The principal components (PCs) were calculated using the scaled data (O<sub>3</sub>, NO, NO<sub>2</sub> and NO<sub>x</sub>) and meteorological variables like solar radiation (SR), temperature (Temp), the sine of wind direction ( $V_x$ ), the cosine of wind direction ( $V_y$ ) and wind speed (WS). The component  $V_x$  of wind direction illustrates air mass movements from the west to east and  $V_y$  component of wind direction illustrates air mass movements from the south to north. The analysis of the post monsoon and winter data set gave two PCs with eigenvalues greater than 1, expressing about 76 % and 72 % of the total variance, respectively. The number of principal components to be retained was decided on the basis of their eigenvalues. PCs with eigenvalues greater than 1 were taken into consideration. Factor loadings greater than 0.5 were considered statistically significant. The principal component profiles were constructed on the basis of factor loadings as shown in Fig. 5.

The principal components (PC1: 44 % and PC2: 43 % in post monsoon; PC1: 34 %, PC2: 29 % and PC3: 22 % in winter) explains approximately 87 % and 85 % of the total variance of the raw data in winter and post monsoon season, respectively. In both the seasons, the first factor (Factor 1)

showed high positive loadings on Temperature, Solar Radiation, Wind Speed and Ozone and high negative loadings on NO, NO<sub>2</sub> and NO<sub>x</sub>. The second and third component showed

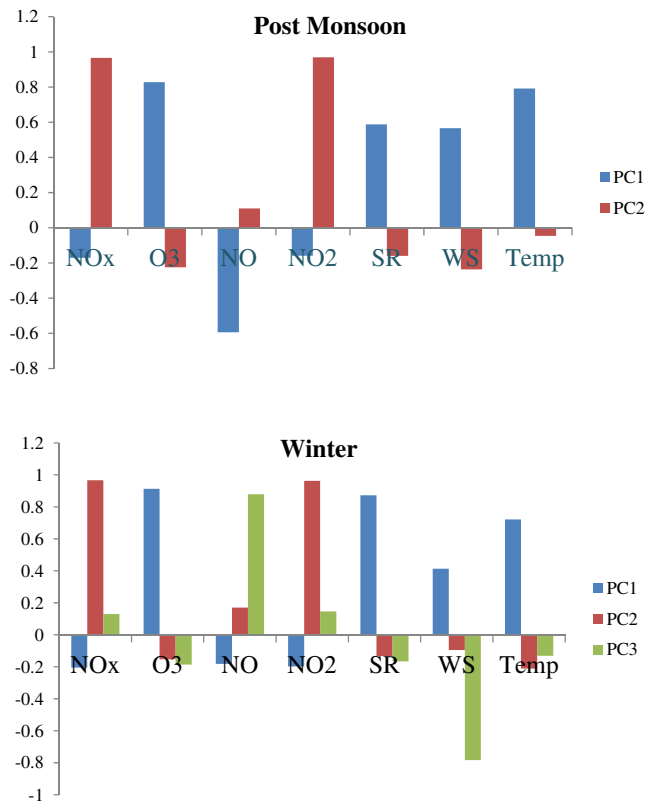


Fig. 5 Principal component profiles on the basis of factor loadings

high loading on NO<sub>2</sub>, NO and NO<sub>x</sub>.  $V_x$  and  $V_y$  components of wind direction were observed to have no contribution to either component. The principal components obtained reveals that the formation of O<sub>3</sub> is governed equally by meteorological parameters (temperature, solar radiation, wind speed) and ozone precursors (NO and NO<sub>2</sub>). In addition to this, factor loadings on principal components also confirms that ozone and meteorological parameters follows inverse relationship with ozone precursors, i.e., NO and NO<sub>2</sub>.

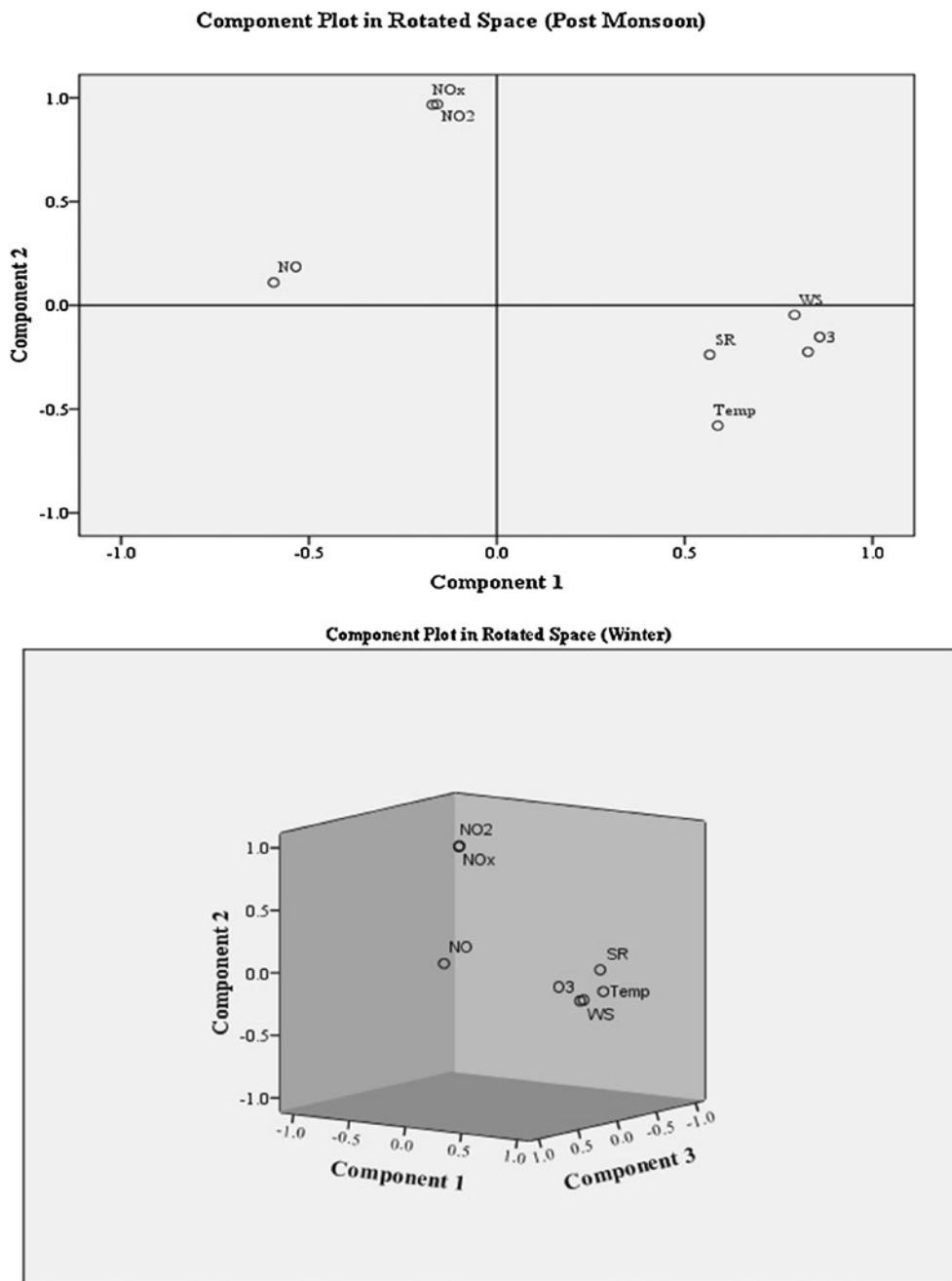
Thus, PCA analysis using O<sub>3</sub> and meteorological parameters (for both periods) showed that ozone concentrations are highly correlated with temperature, solar radiation and

wind speed while O<sub>3</sub> precursors (NO, NO<sub>2</sub> and NO<sub>x</sub>) were observed to be negatively correlated with O<sub>3</sub> (also represented by factor loadings in Fig. 6). Furthermore, to study the contribution of the various sources of variances (PCs) to individual samples, score plots were plotted. Score plots are the projections of the samples in original  $X_1$ – $X_2$  space. The scores are calculated as:

$$S_{i,PCi} = \sum (W_{j,PCj}X_{ij})$$

where  $S_{i,PCi}$  is the score of sample  $i$  on PC1 (principal component 1) and  $W_{j,PCj}$  is the loading of variable  $j$  on

**Fig. 6** Factor loadings PC1 vs. PC2





PC1. Similarly, scores on PC2 are calculated. Figure 7 shows the score plot for post monsoon and winter data set. Samples 269, 539, 608, 624 (post monsoon), 74, 118, 960, 962 (winter) with higher O<sub>3</sub> concentrations represented warm sunny day with relatively higher surface temperature and solar intensity, while samples 218, 284, 698 (post monsoon), 12, 182, 134, 712 (winter) with lower concentrations are relatively cold and wet days and hence show strong dependence of O<sub>3</sub> formation on solar radiation and temperature.

In post monsoon, the averaged data set used for the analysis was windowed for periods of “intense photochemical

activity” and “lesser photochemical activity.” The period with lesser photochemical activity is characterized by heavy rain (98.5–112.5 mm) and cloud cover effects. The periods of intense photochemical activity and lesser photochemical activity may also be referred as sunny days and cloudy days, respectively. From the results of a correlation matrix (Table 1) showing the cross correlations between the different variables used, the more significant relationships for O<sub>3</sub> appeared to be with temperature and solar radiation.

The period with lesser photochemical activity was covered with clouds and a significant decrease in O<sub>3</sub> concentrations

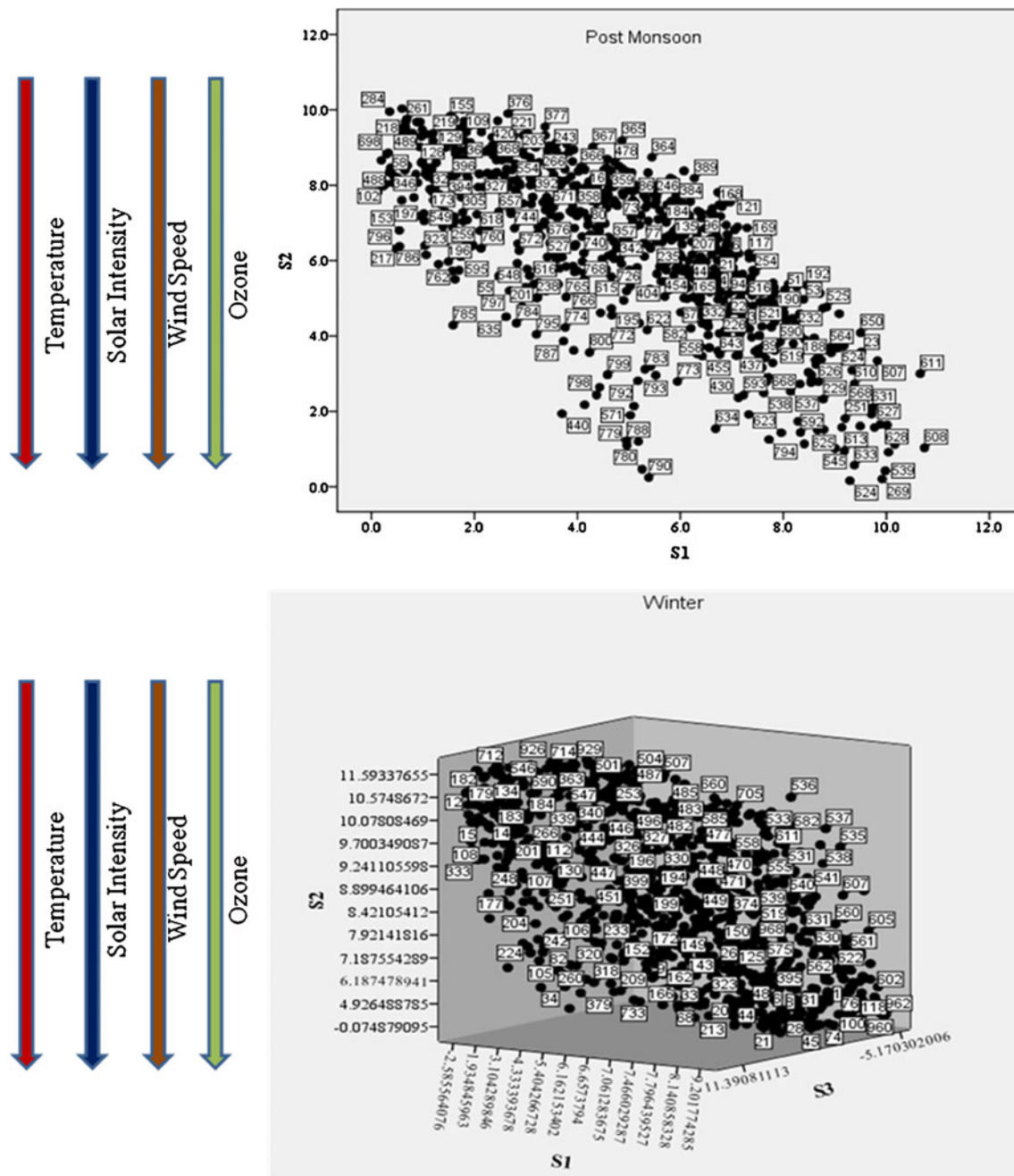


Fig. 7 Score plot, S1 vs. S2 for winter

**Table 1** Correlation matrix

	O <sub>3</sub>	NO <sub>x</sub>	NO	NO <sub>2</sub>	Temp	SR	WS	WS
O <sub>3</sub>	1							
NO <sub>x</sub>	-0.08	1						
NO	-0.27	0.42	1					
NO <sub>2</sub>	-0.04	0.79	0.28	1				
Temp	0.83	-0.24	-0.27	-0.21	1			
SR	0.72	-0.14	-0.16	-0.12	0.69	1		
WS	0.42	-0.45	-0.14	-0.46	0.53	0.48	1	

was observed due to lesser solar radiation, lesser surface temperature and wash out effects. The variations in O<sub>3</sub> concentration as a function of solar radiation, wind speed and relative humidity on cloudy days (September 17–21) and sunny days (September 12–16 and 22–25) are shown in Fig. 8. It is observed that on sunny days, O<sub>3</sub> concentration varies from 25 to 32 ppb when solar radiation (19–23 W m<sup>-2</sup>) is at its maximum and relative humidity ranges from 60 to 85 %. During cloudy days, experiencing the effects of cloud cover, rain (112.5 mm) and lesser solar radiation (1.2–3 W m<sup>-2</sup>), O<sub>3</sub> concentration drops to almost half and is found to vary from 13 to 20 ppb with relative humidity reaching up to 92 %.

Considering solar radiation as one of the important variable playing role in the formation of O<sub>3</sub>, the score plots were drawn to study the contribution of other variables to O<sub>3</sub> formation on cloudy and sunny days (Fig. 9). It is clearly observed from the figure that O<sub>3</sub> concentration increases with increasing solar radiation, temperature and decreasing relative humidity. Therefore on cloudy days with minimum solar radiation, O<sub>3</sub> concentrations are observed to be low and hence are clustered towards lower concentration region. On the other hand, sunny days with high solar radiation and higher surface temperature experiences high O<sub>3</sub> concentration and hence are grouped towards higher concentration region.

### 3.4 Regression model

PCA and CA showed that formation of O<sub>3</sub> is strongly correlated with the prevailing meteorological conditions and concentration of precursor gases. Therefore, MLR was performed to estimate the dependence of ozone concentrations on meteorological parameters and derive a mathematical relationship between O<sub>3</sub>, its precursors and meteorological parameters. MLR analysis was conducted on ozone concentrations for every hour of the day. The original data were standardized before computation in order to avoid misclassifications arising from different orders of magnitude of measured variables. The

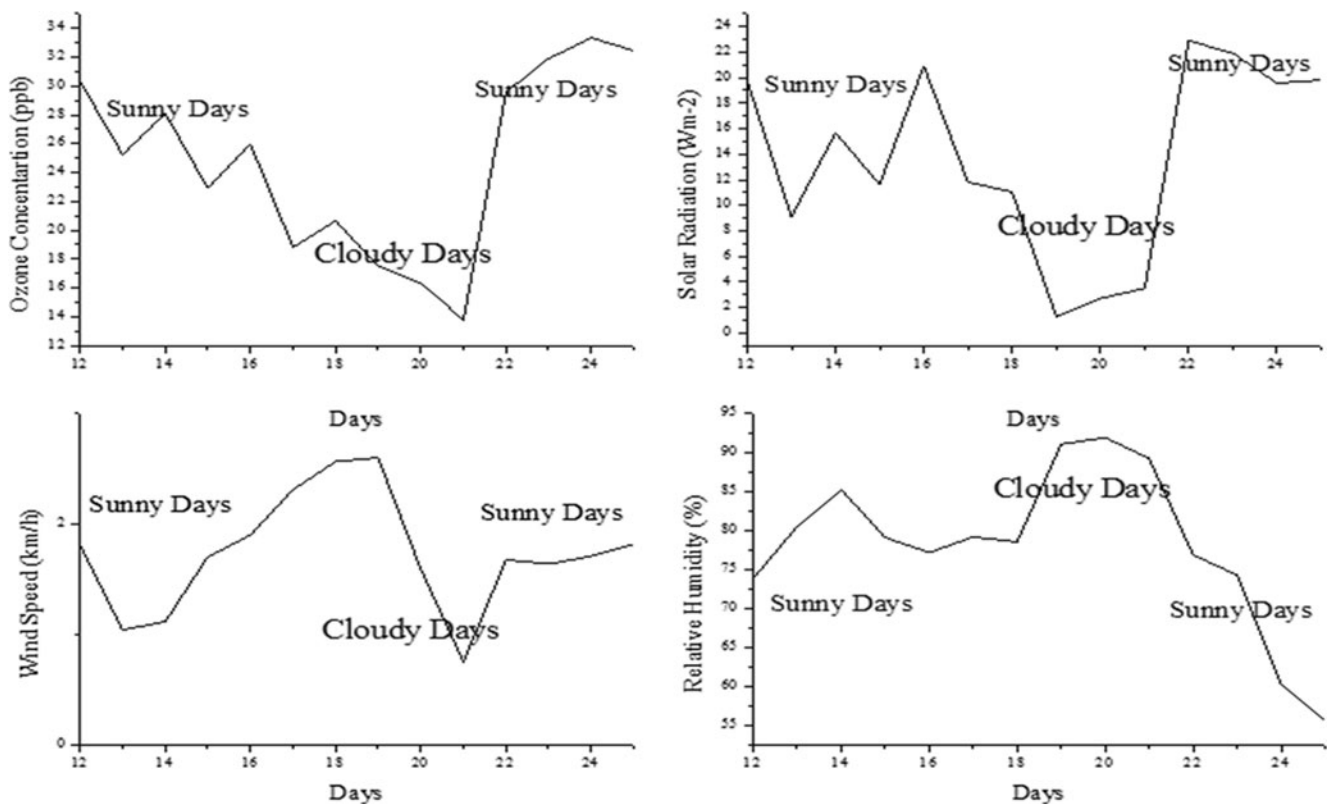


**Fig. 8** Variation of O<sub>3</sub> concentration with solar radiation, wind speed and relative humidity

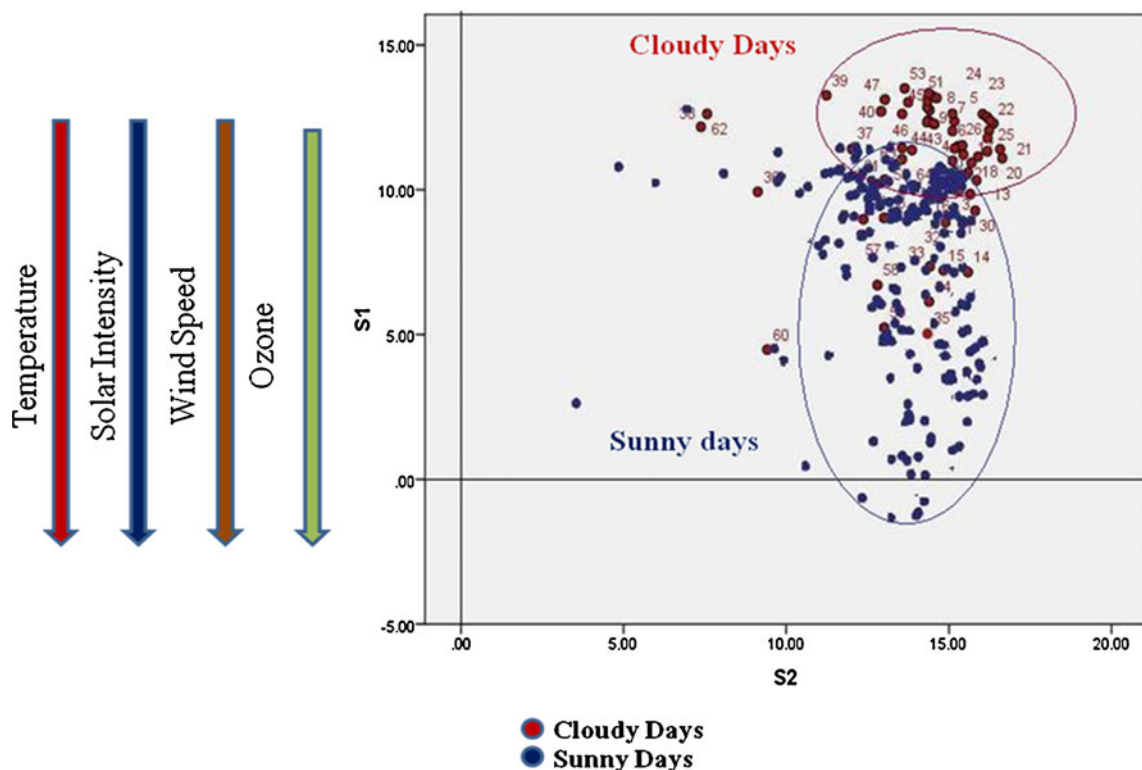


Fig. 9 Score plot, S1 vs. S2 for sunny and cloudy days

data were mean (average) centered and divided by the relevant standard deviations.

Six variables (solar radiation, temperature, wind speed,  $V_x$  and  $V_y$  components of wind) were used as predictor variables in multiple regression analysis. In post monsoon, wind speed and wind direction are not statistically significant and hence the equation obtained is as follows:

$$O_3 = -57.1 + 3.9(\text{Temp}) + 4.9(\text{SR}) - 0.4(\text{NO}_x)$$

Regression analysis using temperature, solar radiation and  $\text{NO}_x$  yielded  $R^2=0.64$ . The ozone concentrations obtained using this equation was plotted against the observed results as shown in Fig. 10. The predicted ozone concentrations showed linear relationship with the observed ozone concentrations.

The same procedure was applied to winter data set. Here wind direction was found to be statistically insignificant and hence yielded the following equation with  $R^2=0.81$ :

$$O_3 = -17.4 + 3.5(\text{Temp}) + 14.8(\text{SR}) + 2.7(\text{WS}) - 0.5(\text{NO}_x)$$

The predicted ozone concentrations using this equation and observed concentrations (Fig. 10) showed linear relationship with each other. Measurements of few VOCs (benzene, toluene and xylene) and polycyclic aromatic compounds (EPA 16 priority PAHs) were also measured at this site. The average concentration of VOCs (BTX) ranged from 2 to

$15 \mu\text{g m}^{-3}$  (Singla et al. 2012), and the total PAH concentration ranged from 15.2 to 392.3  $\text{ng m}^{-3}$  for polycyclic aromatic compounds (Rajput and Lakhani 2010).

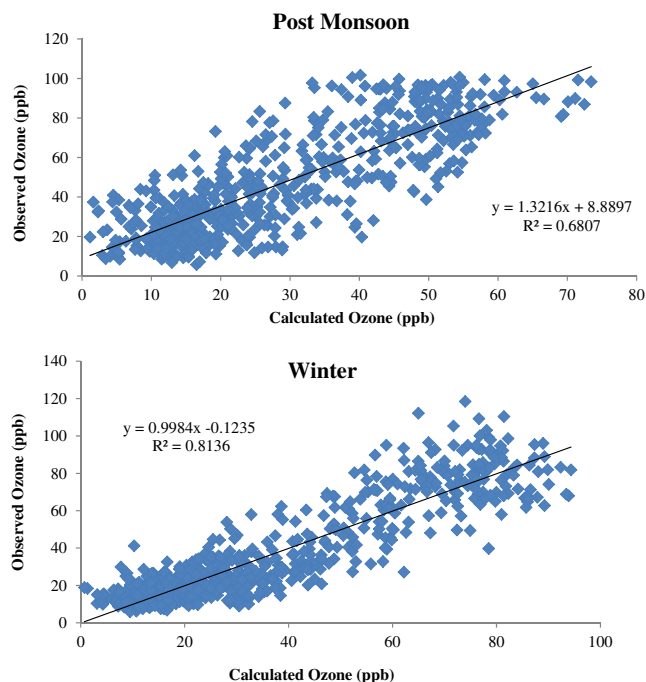
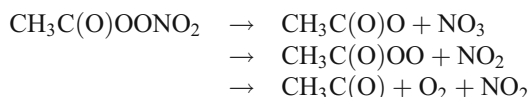


Fig. 10 Ozone concentrations experimentally observed vs. calculated by the regression equation

Of all the meteorological parameters, temperature, solar radiation and wind speed enhance the formation of ozone. Other research groups (Lengyel et al. 2004; Abdul-Wahab et al. 2005; Felipe-Sotelo et al. 2006; Karatzas and Kaltsatos 2007; Andric et al. 2009) have also observed a similar pattern.  $V_x$  and  $V_y$  (sine and cosine of the wind direction) were observed to have no effect on  $O_3$  formation during the study period. Similar result was also observed through PCA. Further, the increase of ozone concentration is also expected to be influenced by temperature which could be attributed to two well-known facts: (1) higher temperatures cause convection to develop, which in turn can enhance vertical ozone transport and (2) dependence of temperature on number of atmospheric reactions. For example, PAN chemistry is reported to be mostly responsible for the dependence of ozone formation on temperature. The photolysis of PAN at higher temperatures yields higher concentration of  $NO_2$  via following set of reactions:



The wavelength thresholds for these at 298 K are 1,025, 990, and 445 nm, respectively. This  $NO_2$  further undergoes photolysis and results in higher ozone production. Few model studies have also reported the enhanced thermal decomposition of peroxyacyl nitrates (PANs) at high temperatures and hence higher ozone yields (Sillman and Samson 1995; Vogel et al. 1999; Baertsch-Ritter et al. 2004). Therefore,  $O_3$  concentration was observed to increase when temperature and solar radiation increase.

#### 4 Conclusion

Surface ozone ( $O_3$ ),  $NO$ ,  $NO_2$ ,  $NO_x$  and few meteorological parameters were measured at Agra (North Central India, 27 °10'N, 78 °05'E) using continuously operating  $O_3$  analyzer (Thermo Fischer Model 49i) and  $NO_x$  analyzer (Thermo Fischer Model 42i) in the post monsoon and winter of 2010. The results of this paper indicate that maximum  $O_3$  formation is observed during daytime due to photo-oxidation of the precursor gases. The average diurnal maximum varied from 43 to 49 ppb in post monsoon during 13:00–15:00 hours and from 66 to 75 ppb in winter during 14:00–16:00 hours. The average diurnal minimum was observed during nighttime and early morning hours ranging from 7 to 13 ppb. Similarly, the average diurnal maximum of  $NO_x$  was observed to vary from 8 to 10 ppb in post monsoon and 10–13 ppb in winter. It was observed that the calculated average 8-h  $O_3$  standard lies below the critical 8-h standard set by EPA. Measurements also show important relationship between changes in meteorology

and  $O_3$  concentration. The calculated equations could be used to predict an estimate of  $O_3$  concentrations with few meteorological parameters. The results of PCAs detected underlying relationships between  $O_3$  concentrations and meteorological data. PCA showed that formation of ozone is equally dependent on ozone precursors and meteorological parameters. Further, regression analysis showed that solar radiation, temperature and wind speed enhanced formation of  $O_3$  while  $O_3$  precursors ( $NO$  and  $NO_2$ ) reduced its concentration.

**Acknowledgments** The authors are thankful to Director, Dayalbagh Educational Institute, Agra and Head, Department of Chemistry for necessary help. They gratefully acknowledge the financial support provided by ISRO-GBP under AT-CTM project. One of the authors, Vyoma Singla, is grateful to the above project for providing JRF.

#### References

- Abdul-Wahab SA, Bakheit CS, Al-Alawi SM (2005) Principal component and multiple regression analysis in modeling of ground-level ozone and factors affecting its concentrations. *Environ Modell Softw* 20:1263–1271
- Andric EK, Brana J, Gvozdic V (2009) Impact of meteorological factors on ozone concentrations modelled by time series analysis and multivariate statistical methods. *Ecol Inf* 4:117–122
- Bai J (2010) Study on surface  $O_3$  chemistry and photochemistry by UV energy conservation. *Atmos Pollut Res* 1:118–127
- Baertsch-Ritter N, Keller J, Dommen J, Prevot ASH (2004) Effects of various meteorological conditions and spatial emission resolutions on the ozone concentration and  $ROG/NO_x$  limitation in the Milan area (I). *Atmos Chem Phys* 4:423–438
- Broniman S, Neu U (1997) Weekend–weekday differences of near-surface ozone concentrations in Switzerland for different meteorological conditions. *Atmos Environ* 31(8):1127–1135
- Cheng KJ, Tsai CH, Chiang HC, Hsu CW (2007) Meteorologically adjusted ground level ozone trends in southern Taiwan. *Environ Monit Assess* 129(1–3):339–347
- Debaje SB, Kakade AD (2009) Surface ozone variability over western Maharashtra, India. *J Hazard Mal* 161:686–700
- Duenas C, Fernandez MC, Canete S, Carretero J, Liger E (2002) Assessment of ozone variations and meteorological effects in an urban area in the Mediterranean Coast. *Sci Tot Environ* 299:97–113
- Elminir HK (2005) Dependence of urban air pollutants on meteorology. *Sci Tot Environ* 350(1–3):225–237
- Felipe-Sotelo M, Gustems L, Hernández I, Terrado M, Tauler R (2006) Investigation of geographical and temporal distribution of tropospheric ozone in Catalonia (North-East Spain) during the period 2000–2004 using multivariate data analysis methods. *Atmos Environ* 40:7421–7436
- Finlayson-Pitts BJ, Pitts JN (1986) Formation of sulfuric and nitric acids in acid rain and fogs. *Atmospheric chemistry: Fundamental and experimental techniques*. John Wiley, New York, pp 702–705
- Ho KF, Lee SC, Chiu GMY (2002) Characterization of selected volatile organic compounds, polycyclic aromatic hydrocarbons and carbonyl compounds at a roadside monitoring station. *Atmos Environ* 36:57–65
- Jackson JE (1991) A users guide to principal components. Wiley-Interscience, John Wiley & Sons, New York, (US). 569 pp.

- Judith P, Pawson S, Ryan L, Fogt J, Nielsen E, Neff WD (2008) Impact of stratospheric ozone hole recovery on Antarctic climate. *Geophys Res Lett* 35:L08714. doi:10.1029/2008GL033317
- Karatzas K, Kaltsatos S (2007) Air pollution modeling with aid of computational intelligence methods in Thessaloniki, Greece. *Simul Modell Pract Theory* 15:1310–1319
- Khiem M, Ooka R, Huang H, Hayami H, Yoshikado H, Kawamoto Y (2010) Analysis of the relationship between changes in meteorological conditions and the variation in summer ozone levels over the Central Kanto area. *Adv Meteorol*, Article ID 349248, 13 pp
- Lal S, Naja M, Subbaraya BH (2000) Seasonal variations in surface ozone and its precursors over an urban site in India. *Atmos Environ* 34:2713–2724
- Relievel J, Crutzen PJ (1990) Influence of cloud photochemical processes on tropospheric ozone. *Nature* 343:227–233
- Lengyel A, Heberger K, Paksy L, Banhidi O, Rajko R (2004) Prediction of ozone concentration in ambient air using multivariate methods. *Chemos* 57:889–896
- Naja M, Lal S (2002) Surface ozone and precursor gases at Gadanki (13.58 °N, 79.28 °E), a tropical rural site in India. *J Geophys Res* 107 (D14). doi:10.1029/2001JD000357
- Pudasainee D, Sapkota B, Shrestha ML, Kaga A, Kondo A, Inou Y (2006) Ground level ozone concentrations and its association with NO<sub>x</sub> and meteorological parameters in Kathmandu valley, Nepal. *Atmos Environ* 40:8081–8087
- Rajput N, Lakhani A (2010) Measurements of polycyclic aromatic hydrocarbons in an urban atmosphere of Agra, India. *Atmosfera* 23(2):165–183
- Roemer M, Tarasova O (2002) Methane in The Netherlands – an exploratory study to separate time scales. TNO report R 2002/215, The Netherlands
- Scheel HE, Areskoung H, Geiss H, Gomisichel B, Granby K, Haszpra L, Klasink L, Kley D, Laurila T, Lindskog T, Roemer M, Schmitt R, Simmonds P, Solberg S, Toupance G (1997) On the spatial distribution and seasonal variation of lower-troposphere ozone over Europe. *J Atmos Chem* 28:11–28
- Singla V, Pachauri T, Satsangi A, Kumari KM, Lakhani A (2012) Comparison of BTX Profiles and their Mutagenicity Assessment at two sites of Agra, India. *Sci World J*. doi:10.1100/2012/272853
- Sillman S, Samson PJ (1995) Impact of temperature on oxidant photochemistry in urban, polluted and remote environments. *J Geophys Res* 100:11 497–11 508
- Son SW, Polyvani LM, Waugh DW, Akiyoshi H, Garcia R, Kinnison D, Pawson S, Rozanov E, Shepherd TG, Shibata K (2008) The impact of stratospheric ozone recovery on the Southern Hemisphere westerly jet. *Sci* 320:1486–1489
- Spichtinger N, Winterhalter M, Fabian P (1996) Ozone and Grosswetterlagen: analysis for the Munich Metropolitan Area. *Environ Sci Poll Res* 3(3):145–152
- Statheropoulos M, Vassiliadis N, Pappa A (1998) Principal component and canonical correlation analysis for examining air pollution and meteorological data. *Atmos Environ* 32(6):1087–1095
- Tarasova OA, Karpetchko AY (2003) Accounting for local meteorological effects in the ozone time-series of Lovozero (Kola Peninsula). *Atmos Chem Phys Discuss* 3(655):676
- Tu J, Xia ZG, Wang H, Li W (2007) Temporal variations in surface ozone and its precursors and meteorological effects at an urban site in China. *Atmos Res* 85(3–4):310–337
- Vogel B, Riemer N, Vogel H, Fiedler F (1999) Findings on NO<sub>y</sub> as an indicator for ozone sensitivity based on different numerical simulations. *J Geophys Res* 104:3605–3620
- Wilson SR, Solomon KR, Tang X (2007) Changes in tropospheric composition and air quality due to stratospheric ozone depletion and climate change. *PPS* 6:301–310
- Winer AM, Peters JW, Smith JP, Pitts JN Jr (1974) Response of commercial chemiluminescent NO–NO<sub>2</sub> analyzers to other nitrogen-containing compounds. *Environ Sci Technol* 8:1118–1121